[CANCER RESEARCH 64, 4547–4554, July 1, 2004]

AML1-ETO Decreases ETO-2 (MTG16) Interactions with Nuclear Receptor Corepressor, an Effect That Impairs Granulocyte Differentiation

Vinzon Ibañez,[1] Arun Sharma,[1] Silvia Buonamici,[1] Amit Verma,[1] Sudhakar Kalakonda,[3] Jianxiang Wang,[4] ShriHari Kadkol,[2] and Yogen Saunthararajah[1]

[1]Section of Hematology/Oncology, Department of Medicine, and [2]Department of Pathology, University of Illinois, Chicago, Illinois; [3]Department of Ophthalmology, University of Maryland, Baltimore, Maryland; and [4]Laboratory of Hematological Malignancy, State Key Laboratory of Experimental Hematology, Institute of Hematology, Chinese Academy of Medical Sciences

ABSTRACT

The t(8;21) chromosome abnormality in acute myeloid leukemia targets the *AML1* and *ETO* genes to produce the leukemia fusion protein AML1-ETO. Another member of the ETO family, ETO-2/MTG16, is highly expressed in murine and human hematopoietic cells, bears >75% homology to ETO, and like ETO, contains a conserved MYND domain that interacts with the nuclear receptor corepressor (N-CoR). AML1-ETO prevents granulocyte but not macrophage differentiation of murine 32Dcl3 granulocyte/macrophage progenitors. One possible mechanism is recruitment of N-CoR to aberrantly repress AML1 target genes. We wished to examine another mechanism by which AML1-ETO might impair granulocyte differentiation. We demonstrate that AML1-ETO decreases interactions between ETO-2 and N-CoR. Furthermore, overexpression of ETO-2 relieves AML1-ETO-induced granulocyte differentiation arrest. This suggests that decreased interactions between ETO-2 and N-CoR may contribute to granulocyte differentiation impairment. The MYND domain coimmunoprecipitates with N-CoR and inhibits interactions between ETO-2 and N-CoR, presumably by occupying the ETO-2 binding site on N-CoR. This inhibition of ETO-2 interactions with N-CoR is specific because the MYND domain does not inhibit retinoic acid receptor interactions with N-CoR. To examine the effect of decreasing interactions between ETO-2 and N-CoR in hematopoietic cells, without effects of AML1-ETO such as direct repression of AML1 target genes, the MYND domain was expressed in 32Dcl3 and human CD34+ cells. The MYND domain prevented granulocyte but not macrophage differentiation of both 32Dcl3 and human CD34+ cells, recapitulating this effect of AML1-ETO. In conclusion, decreasing interactions between ETO-2 and N-CoR, an effect of AML1-ETO, inhibits granulocyte differentiation.

INTRODUCTION

MTG16 (murine homologue ETO-2) is a member of the ETO family; the other members are MTG8 (ETO) and MTGR1. MTG16/ETO-2 is expressed in hematopoietic cells. Murine ETO-2 bears 75% identity with murine ETO, 86% identity with human MTG16, and 77% identity with human ETO (1). Both *MTG16* and *ETO* are targets of chromosomal translocations in acute myeloid leukemia, the t(16;21) and t(8;21) abnormalities, respectively. Both ETO-2 and ETO interact with nuclear receptor corepressor (N-CoR); the usual function of this interaction is not known.

There are four regions conserved among the ETO family members, typically referred to as the nervy homology regions (NHR) after nervy, the ETO homologue found in *Drosophila*. NHR1 has sequence similarity with a central domain found in human TAF105, human TAF130 and Drosophila Taf110—it is also known as the TAF homology domain. NHR2 is an amphipathic helix structure that mediates homodimerization and binding of ETO to homologous family members (2). NHR3 is a coiled-coiled region that plays a role in interactions with N-CoR (3). NHR4 contains two MYND zinc finger motifs, which are necessary for binding to N-CoR (3–7); it is also known as the MYND domain.

ETO-2, like ETO, demonstrates corepressor function (8). This function is likely to be mediated through the interactions of ETO-2 with histone deacetylases 1, 2, 3, 6, and 8 and the ubiquitously expressed N-CoR. N-CoR is a large (2440 amino acids) platform protein known to mediate transcriptional repression by unliganded nuclear receptors and many other classes of transcription factors. N-CoR function is mediated at least in part through its interactions with Sin3-histone deacetylase (9, 10). Some of N-CoR function in hematopoiesis is mediated by its interactions with the retinoic acid receptor (RAR) and the thyroid hormone receptor (11, 12). N-CoR interaction with unliganded RAR is suggested to block maturation of granulocytes (12, 13).

MTG16 is highly expressed in human heart, pancreas, skeletal muscle, spleen, thymus, and peripheral blood leukocytes (14). ETO-2 is expressed in murine heart, brain, spleen, lung, liver, muscle, and kidney (1).

Acute myeloid leukemia containing chromosomal translocations involving ETO and MTG16 usually have an acute myeloblastic leukemia with maturation (FAB M2) phenotype. We demonstrate that AML1-ETO, the leukemia fusion protein produced by the t(8;21) abnormality, decreases interactions between ETO-2 and N-CoR. After confirming that a 77-amino acid ETO fragment containing the MYND domain could decrease ETO-2 interactions with N-CoR in 293T cells (presumably by competing with ETO-2 for binding to the same interaction site on N-CoR), we expressed this fragment in hematopoietic cells. The MYND fragment was sufficient to inhibit granulocyte differentiation of murine 32Dcl3 and human CD34+ hematopoietic cells, recapitulating this effect of AML1-ETO. This suggests that disruption of endogenous ETO-2 interactions with N-CoR may be a relevant leukemogenic effect of the AML1-ETO leukemia fusion protein.

MATERIALS AND METHODS

Reverse Transcription-PCR. Total RNA was extracted by the RNeasy Mini Kit (Qiagen, Valencia, CA) according to the manufacturer's protocol. On-column DNase I digestion was performed to eliminate genomic DNA contamination. Absence of DNA in purified RNA was confirmed by PCR amplication without reverse transcription. ETO, ETO-2, and glyceraldehyde-3-phosphate dehydrogenase expression was analyzed using the One Step reverse transcription-PCR kit (Qiagen) in a MJ Research PTC 200 DNA Engine thermocycler. Each reaction contained 1 μg of total RNA; 1× reverse transcription-PCR buffer (with 2.5 mM $MgCl_2$); 0.4 mM each of dATP, dCTP, dTTP, and dGTP; 1× Q solution; 30 pmol each of forward and reverse primers; 10 units of RNase inhibitor (Promega); and 2 μl of enzyme mix containing reverse transcriptase and HotStarTaq DNA polymerase. Primer sequences were designed and optimized using Oligo Version 6.0 software (Molecular Biology Insights, CO). Primer sequences were: ETO (human and

Received 11/25/03; revised 4/9/04; accepted 4/26/04.

Grant support: Illinois Department of Public Health/UIC Sickle Cell Center and the American Cancer Society (Y. Saunthararajah), National Natural Science Foundation of China Grant 30370593 (J. Wang), National Science Fund for Distinguished Young Scholars Grant 30025019, and Tianjin Natural Science Fund Grant 003803211.

The costs of publication of this article were defrayed in part by the payment of page charges. This article must therefore be hereby marked *advertisement* in accordance with 18 U.S.C. Section 1734 solely to indicate this fact.

Requests for reprints: Yogen Saunthararajah, MBRB room 3150 (MC734), 900 South Ashland Avenue, Chicago, IL 60607-7173. Phone: (312) 413-1790; Fax: (312) 413-7963; E-mail: yogen@uic.edu.

mouse) forward, 5′-CCA GCG GTA CAG TCC AAA T-3′; reverse, 5′-CTR GAG TGG CTG CTG CTA CT-3′; ETO-2 (mouse) forward, 5′-ACG GCC TCG CTC TCC AC-3′; reverse, 5′-GGT GCA GGA CCG CTT ACT G-3′; MTG16 (human) forward, 5′-CGG GAG CTA CGA GAG C-3′; reverse, 5′-CGT AGC CGG TGA GGG T-3′. Reverse transcription was performed at 48° for 1 h followed by heat inactivation of the reverse transcriptase at 95° for 15 min. This step simultaneously activated the HotStarTaq DNA polymerase. PCR amplification was subsequently performed for 28 cycles and 34 or 40 cycles. Each cycle consisted of denaturation at 92° for 30 s, annealing at 60° for 30 s, and extension at 72° for 40 s. After a final extension at 72° for 10 min, the reactions were chilled to 4°. Ten μl of each reverse transcription-PCR product were electrophoresed on a 2% agarose gel (E-gel; Invitrogen), and the gel image was captured digitally using the AlphaImager IS-3400 System (α Innotech). Images were acquired under nonsaturating conditions. The gel images are shown in reverse contrast to enhance clarity.

Cloning. A nuclear-localizing signal fused to a myc-tag was subcloned from the pCMV/myc/nuc expression vector (Invitrogen) into the *Sal*I/*Bam*HI site on pIRES-EGFP2 (Clontech). The ETO MYND zinc finger domain from amino acids 484–560 (GenBank accession no. D14289) was cloned into the *Xho*I/*Sal*I site of the modified pIRES-EGFP2 (forward primer, 5′-agt tgc tgg aat tgt ctc gag aaa gag agt-3′; reverse primer, 5′-g agg ggt tgt cgt cga cgt gga-3′). The ETO MYND zinc finger domain was also cloned into the MSCV retroviral vector (Clontech; forward primer, 5′-aaa aaa gaa ttc atg aaa gcg agt gaa acc tgc agt ggc-3′; reverse primer, 5′-aaa aaa ctc gag tta gga agg ggt tcc cgg ggt g-3′) modified to replace the G418 resistance cassette with an internal ribosome entry site (IRES)-yellow fluorescent protein (YFP) motif.

Full-length AML1-ETO was also cloned into the MSCV-IRES YFP retroviral vector (forward primer, 5′-aaa aaa gaa ttc atg aaa gcg agt gaa acc tgc agt ggc-3′; reverse primer, 5′-aaa aaa ctc gag tta gga agg ggt tcc cgg ggt g-3′).

Electroporation and Culture of 32Dcl3 Cells. 32Dcl3 cells were electroporated at 280V/950uF using a Bio-Rad Gene Pulser II. Stable transfectants were maintained in murine interleulin-3 (mIL-3) 10 ng/ml (R&D Systems) and selected in G418 for 2 weeks or puromycin for 1 week with subsequent flow sorting for GFP or YFP-positive cells. Repeat experiments included repeat transfection and sorting of a new polyclonal stable transfectant population. For each experiment, 5–10 million stable transfectants were cultured in granulocyte colony-stimulating factor (G-CSF; 50 ng/ml; Amgen) or murine granulocyte-macrophage CSF (mGM-CSF; 10 ng/ml; Peprotech) after four washes in 50 ml of PBS to remove mIL-3.

Retroviral Transduction of Murine 32Dcl3 Cells. The BOSC line was used to package the retrovirus to transfect 32Dcl3 cells. Retrovirus-containing supernatant was added to 32Dcl3 cells in retronectin (TaKaRa)-coated plates. YFP-positive cells were then flow-sorted and expanded in mIL-3.

Retroviral Transduction and Culture of Cord Blood CD34 Cells. The PG13 line was used to package the retrovirus. Retrovirus-containing supernatant was added to human cord blood CD34-positive cells (AllCells) in retronectin (TaKaRa)-coated plates. The cord blood cells were cultured in Iscove's modified Dulbecco's medium (IMDM) 20% FBS (HyClone) containing 30 ng/ml stem cell factor, flt-3 ligand, and thrombopoietin for 48 h before and after retroviral transduction. YFP-positive cells were then flow-sorted before culture in methylcellulose (1×10^3 cells/ml; Stem Cell Technologies, MethoCult H4434) and liquid culture in IMDM 20% FBS containing 30 ng/ml stem cell factor, 30 ng/ml interleukin-3 (IL-3), and 50 ng/ml G-CSF (Amgen).

Flow-Cytometric Analysis and Sorting. 32Dcl3 cells ($1–5 \times 10^6$) were stained for 20 min on ice with anti-GR-1 PE, anti-CD11b, or anti-CD13 (BD-PharMingen) or isotype control (BD-PharMingen); washed once with 3 ml of PBS; and then analyzed using a Becton Dickinson FacsCalibur. A total of 10–30,000 events were analyzed per sample. Cells were flow-sorted using the Becton-Dickinson FacsVantage.

Cytospin Preparations. Cells were spun down onto glass slides at 500 rpm for 5 min using a Shandon Cytospin3 and stained with Giemsa, and photomicrographs were obtained at ×400–630 magnification using a Zeiss microscope.

Cell Counts. Cell counts were performed using trypan blue exclusion and a Neubauer hematocytometer (Hausser Scientific).

Immunoprecipitations and Western Blotting. Approximately 50 million cells (all of 100-mm plate if adherent) were spun down, and the pellet was lysed in 700 μl of cold lysis buffer [25 mM Tris-Cl (pH 7.5), 150 mM NaCl, and 1.0% IGEPAL] or cold EBC lysis buffer [50 mM Tris-CL (pH 7.5), 120 mM NaCl, and 0.5% IGEPAL]. The lysate was spun at 14,000 rpm at 4°C after incubation in ice for 30 min (or 2 h of incubation at 4°C with constant agitation in the case of cells lysed with EBC lysis buffer). The lysate was incubated with 2–4 μg of antibody for 2 h at 4°C (100 μl of lysate were retained for direct loading onto gel). Then, 30 μl of protein G Sepharose (Zymed) were added followed by incubation for another 2 h or overnight at 4°C. The beads were washed with wash buffer [50 mM Tris-Cl (pH 8.0), 150 mM NaCl, 1 mM EDTA, and 0.1% IGEPAL] ×3. The beads were then boiled in loading buffer at 95°C for 5 min before loading onto gels. Proteins were separated with SDS-PAGE and transferred onto polyvinylidene difluoride. Residual binding sites on the filters were blocked by incubating with 5% nonfat milk in 90 mM NaCl, 3 mM KCl, 7 mM Na_2PO_4, 1.5 mM KH_2PO_4, and 0.1% Tween 20 for 1 h at room temperature. After incubation with primary and secondary antibodies, the filters were developed using an enhanced chemiluminescence kit (ECL; Amersham Biosciences). Antibodies from Santa Cruz Biotechnology follow: ETO (SC-9737); ETO-2 (SC-9741); RARα (SC-551); N-CoR (SC-1609); Myc 9E10 epitope (SC-40). Antibodies from Sigma follow: HA tag (H-6908); Flag tag (F-3165).

RESULTS

ETO-2 (MTG16) Is Expressed in Murine and Human Hematopoietic Cells. The 32Dcl3 cell line is a murine granulocyte/macrophage progenitor cell line. It is mIL-3 dependent for survival and proliferation. Upon removal of mIL-3, it terminally differentiates into granulocytes in G-CSF and macrophages and granulocytes in mGM-CSF (15). In 32Dcl3 cells (Fig. 1*A*), *ETO-2* expression was demonstrated by reverse transcription-PCR (Fig. 1*A*) and by Western blot (Fig. 1*B*). *ETO* signal was not detected in the 32Dcl3 cells by reverse transcription-PCR (Fig. 1*A*). In human CD34+ hematopoietic cells,

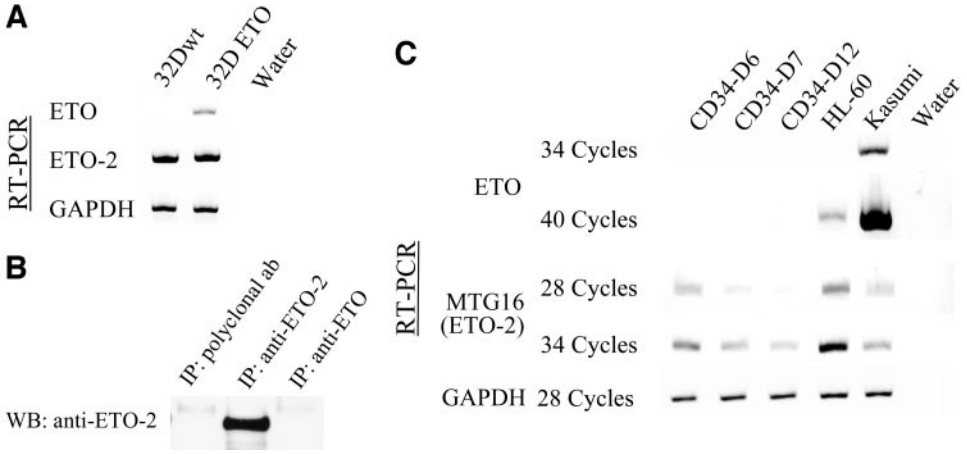

Fig. 1. ETO-2 is expressed in 32Dcl3 cells, human CD34+ hematopoietic cells, HL60 cells, and Kasumi-1 cells. *A*, using reverse transcription-PCR (*RT-PCR*) with primers specific for *ETO* or *ETO-2*, *ETO-2* signal was readily detected in 32Dcl3 wild-type (*32Dwt*) cells. 32Dcl3 cells transfected with an expression vector for ETO (*32D ETO*) were used as a positive control. *B*, 32Dcl3 lysates were immunoprecipitated (*IP*) with nonspecific polyclonal antibody, anti-ETO-2, and anti-ETO. The blot was probed with anti-ETO-2. *C*, RNA was extracted from human CD34+ cells cultured in IMDM supplemented with bovine growth serum and cytokines at D6, D7, and D12, from the myeloid leukemia cell line HL60 and the AML1-ETO-containing cell line Kasumi-1. *MTG16* (*ETO-2*) signal was detected in all of the samples tested; *ETO* was detected in HL60 and Kasumi cells only. In Kasumi cells, the primers for *ETO* would also amplify from *AML1-ETO* transcripts.

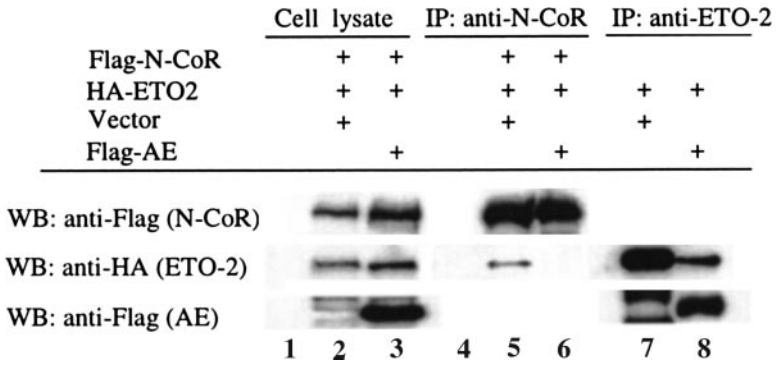

Fig. 2. AML1-ETO (*AE*) decreases the coimmunoprecipitation of ETO-2 with N-CoR. 293T cells were transfected with expression vectors for N-CoR, ETO-2, and either AML1-ETO (*Lanes 3* and *6*) or its empty vector (*Lanes 2* and *5*). Lysates were immunoprecipitated with anti-N-CoR. AML1-ETO prevented the coimmunoprecipitation of ETO-2 with N-CoR (*Lane 6*). AML1-ETO coimmunoprecipitates with ETO-2 (*Lane 8*). *Lanes 1* and *4*, untransfected 293-T lysate. *IP*, immunoprecipitation.

HL60, and Kasumi-1 myeloid leukemia lines, *MTG16* (*ETO-2*) expression was demonstrated by reverse transcription-PCR (Fig. 1*C*). *ETO* signal was not detected in the human CD34+ cells but was detected in the HL60 and Kasumi-1 cells. In the Kasumi-1 cells, the detected *ETO* signal could also have arisen from *AML1-ETO* transcripts (Fig. 1*C*).

AML1-ETO Decreases the Interaction of ETO-2 with N-CoR. Both AML1-ETO and ETO-2 bind to N-CoR (8). We hypothesized that one action of AML1-ETO might be to decrease ETO-2 interactions with N-CoR, through binding/sequestering of ETO-2 or by competing for the same binding site on N-CoR. 293T cells were transfected with equivalent microgram quantities of expression vectors for HA-ETO-2, Flag-NCoR, and either AML1-ETO or its empty vector. The cell lysates were immunoprecipitated with anti-N-CoR, and the blots were probed for HA tagged ETO-2. AML1-ETO prevented the coimmunoprecipitation of ETO-2 with N-CoR. The decreased coimmunoprecipitation of ETO-2 with N-CoR in the presence of AML1-ETO was not a consequence of lower expression of ETO-2 or N-CoR in the AML1-ETO-containing samples (Fig. 2). As reported by others (16), AML1-ETO coimmunoprecipitates with ETO-2 (Fig. 2, *Lane 8*).

ETO-2 Overexpression Relieves the Granulocyte Differentiation Arrest Induced by AML1-ETO Expression in 32Dcl3 Cells. Unlike wild-type 32Dcl3 cells, 32Dcl3 cells transduced with AML1-ETO (32D AML1-ETO) do not terminally differentiate in G-CSF but instead continue to proliferate (15, 17). 32Dcl3 cells were transduced with MSCV AML1-ETO-IRES-YFP (both AML1-ETO and YFP are translated from the same mRNA transcript) or the empty vector. We noted that 32D AML1-ETO cells do not terminally differentiate in G-CSF, as observed by others, but do terminally differentiate into macrophages in mGM-CSF (data not shown). ETO-2 was overexpressed in 32D AML1-ETO cells through transfection with an expres-

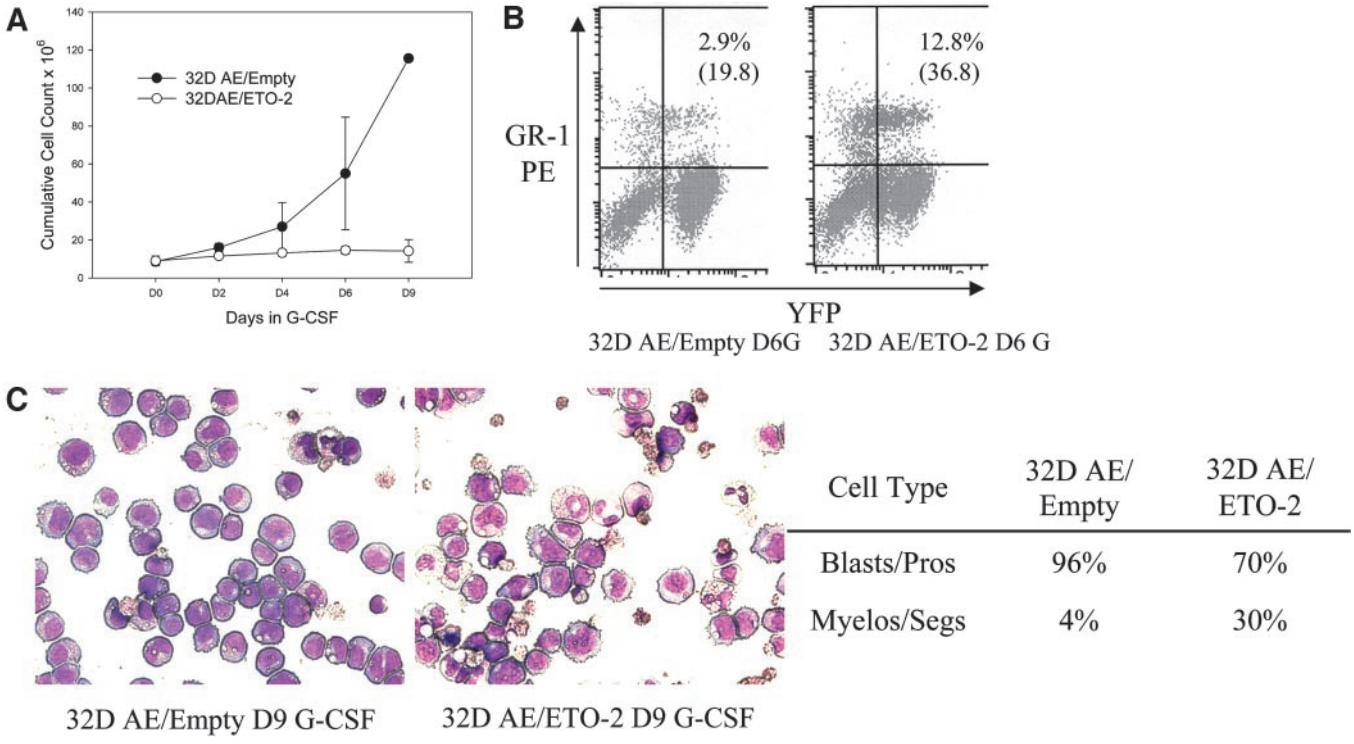

Cell Type	32D AE/ Empty	32D AE/ ETO-2
Blasts/Pros	96%	70%
Myelos/Segs	4%	30%

Fig. 3. ETO-2 relieves the differentiation arrest produced by AML1-ETO (*AE*) in 32Dcl3 cells. 32Dcl3 cells were transduced with MSCV-AML1-ETO-IRES-YFP (*32D AE*). YFP-positive cells were flow-sorted and then transfected with a pCMV expression vector for ETO-2 (*32D AE/ETO-2*) or the empty vector (*32D AE/Empty*). Stable double transfectants were selected in G418. *A*, cell counts of 32D AE/Empty and 32D AE/ETO-2 in G-CSF (mean ± SD of two independent experiments using independently generated polyclonal populations). *B*, GR-1 PE expression (*Y* axis; a murine differentiation marker that increases with granulocyte or monocyte differentiation) on 32D AE/Empty and 32D AE/ETO-2 at day 6 of culture in G-CSF. The *numbers* represent the percentage of live cells by forward-scatter side scatter that are GR-1 positive with the mean fluorescence intensity GR1-PE expression of the YFP-positive cells in parentheses. *C*, Giemsa-stained cytospin preparations of 32D AE/Empty and 32D AE/ETO-2 after 9 days of culture in G-CSF (magnification, ×400).

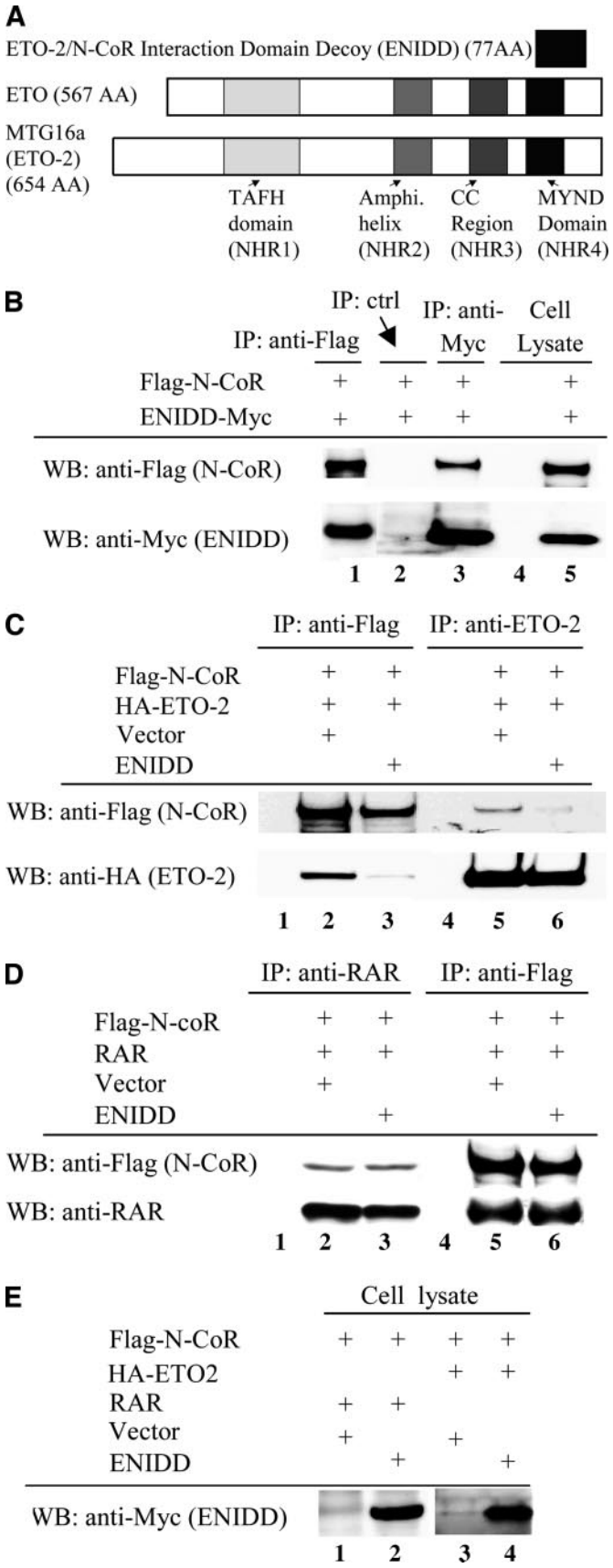

Fig. 4 ENIDD decreases the bidirectional coimmunoprecipitation of Flag-N-CoR with ETO-2-HA but not with the RAR. *A*, human ETO (GenBank accession no. D14289) and human MTG16a (accession no. ABB010419) showing conserved domains (*NHR*, nervy homology region; *TAFH*, TAF homology domain; *amphi.*, amphipathic helix; *CC*, coiled-coiled region). The MYND domain of ETO, or ENIDD (amino acid numbers 484–560), is the domain used to competitively inhibit ETO-2 interaction with N-CoR in these experiments. *B*, Myc-tagged ENIDD (the ETO MYND domain) coimmunoprecipitates bidirectionally with Flag-N-CoR from transfected 293T cells (*Lanes 1* and *3*). *ctrl*, nonspecific polyclonal mouse antibody (*Lane 2*). *C*, 293T cells were transfected with expression vectors for Flag-N-CoR, HA-ETO-2, and either ENIDD-Myc (*Lanes 3* and *6*) or empty vector (*Lanes 2* and *5*). With antiflag immunoprecipitation, there is an equivalent amount of Flag-N-CoR in the 293T lysates but less coimmunoprecipitation of ETO-2-HA in the presence of ENIDD (*Lane 3*). With anti-ETO-2 immunoprecipitation from the same cell lysates, there is an equivalent amount of HA-ETO-2 but less coimmunoprecipitation of Flag-N-CoR in the presence of ENIDD (*Lane 6*). *D*, 293T cells were transfected with expression vectors for Flag-N-CoR, RAR, and either ENIDD-Myc (*Lanes 3* and *6*) or empty vector (*Lanes 2* and *5*). With antiflag immunoprecipitation, there is an equivalent amount of RAR coimmunoprecipitation, even in the presence of ENIDD (*Lane 6*). The same results are seen with anti-RAR immunoprecipitation (*Lane 3*). *E*, ENIDD expression was confirmed by anti-Myc Western blot of cell lysates.

sion vector for ETO-2 (32D AE/ETO-2) or empty vector (32D AE/Empty) and then selection for stable transfectants in G418. ETO-2 overexpression renewed granulocyte differentiation of 32D AML1-ETO cells as demonstrated by cell counts, flow cytometric evaluation for the murine granulocyte differentiation marker GR-1, and cell morphology on Giemsa-stained cytospin preparations (Fig. 3). This suggests that AML1-ETO disruption of usual ETO-2 function may have a role in producing granulocyte differentiation arrest. The experiment was performed in triplicate using three independently generated polyclonal populations of stable transfectants.

At 16 h after initiating culture in G-CSF, 32D AML1-ETO/ETO-2 cells demonstrated G_1 arrest compared with 32D AML1-ETO/Empty. There was no increase in the sub-G_1 fraction at 16 h or at 72 h after culture in G-CSF, suggesting that the decreased cell-cycle progression was a consequence of G_1 arrest without apoptosis (data not shown). It is possible that ETO-2 directly inhibits cell-cycle progression of 32D AML1-ETO cells independent of G_1 arrest associated with differentiation.

32Dcl3 cells transfected with ETO-2 alone (32D ETO-2) did not demonstrate altered differentiation or proliferation in G-CSF (data not shown).

The MYND Domain Alone [ETO/N-CoR Interaction-Domain Decoy (ENIDD)] Binds to N-CoR and Specifically Decreases the Bidirectional Coimmunoprecipitation of ETO-2 with N-CoR. Previously, we and others demonstrated that the MYND domain of ETO (Fig. 4*A*) could bind to NCoR in two-hybrid assays (5, 18). We confirmed that the MYND domain alone (amino-acids 484–560; GenBank accession no. D14289) could coimmunoprecipitate with N-CoR in 293T cells (Fig. 4*B*). We reasoned that the MYND domain, if expressed in cells, would compete with endogenous ETO-2 for binding to the same interaction site on N-CoR. This would allow us to specifically examine the consequences of disrupting endogenous ETO-2 interactions with N-CoR without other effects of full-length AML1-ETO such as direct repression of *AML1* target genes. To reflect our goal of competitively inhibiting endogenous ETO-2 interactions with N-CoR, we termed the MYND zinc finger domain of ETO that we expressed in cells the ENIDD.

To confirm that ENIDD would decrease ETO-2 interactions with N-CoR, 293T cells were transfected with equivalent microgram quantities of expression vectors for HA-ETO-2, Flag-NCoR, and either ENIDD-Myc or its empty vector. The cell lysates were immunoprecipitated with antiflag or anti-ETO-2. ENIDD decreased the bidirectional coimmunoprecipitation of ETO-2 with N-CoR. The decreased coimmunoprecipitation of ETO-2 with N-CoR (and *vice versa*) was not a consequence of lower expression of ETO-2 or N-CoR in the ENIDD-containing samples (Fig. 4*C*). ENIDD did not decrease the bidirectional coimmunoprecipitation of RARα with N-CoR. Therefore, ENIDD was a specific antagonist of ETO-2 interactions with N-CoR (Fig. 4*D*). ENIDD expression was confirmed by anti-myc Western blot of cell lysates (Fig. 4*E*).

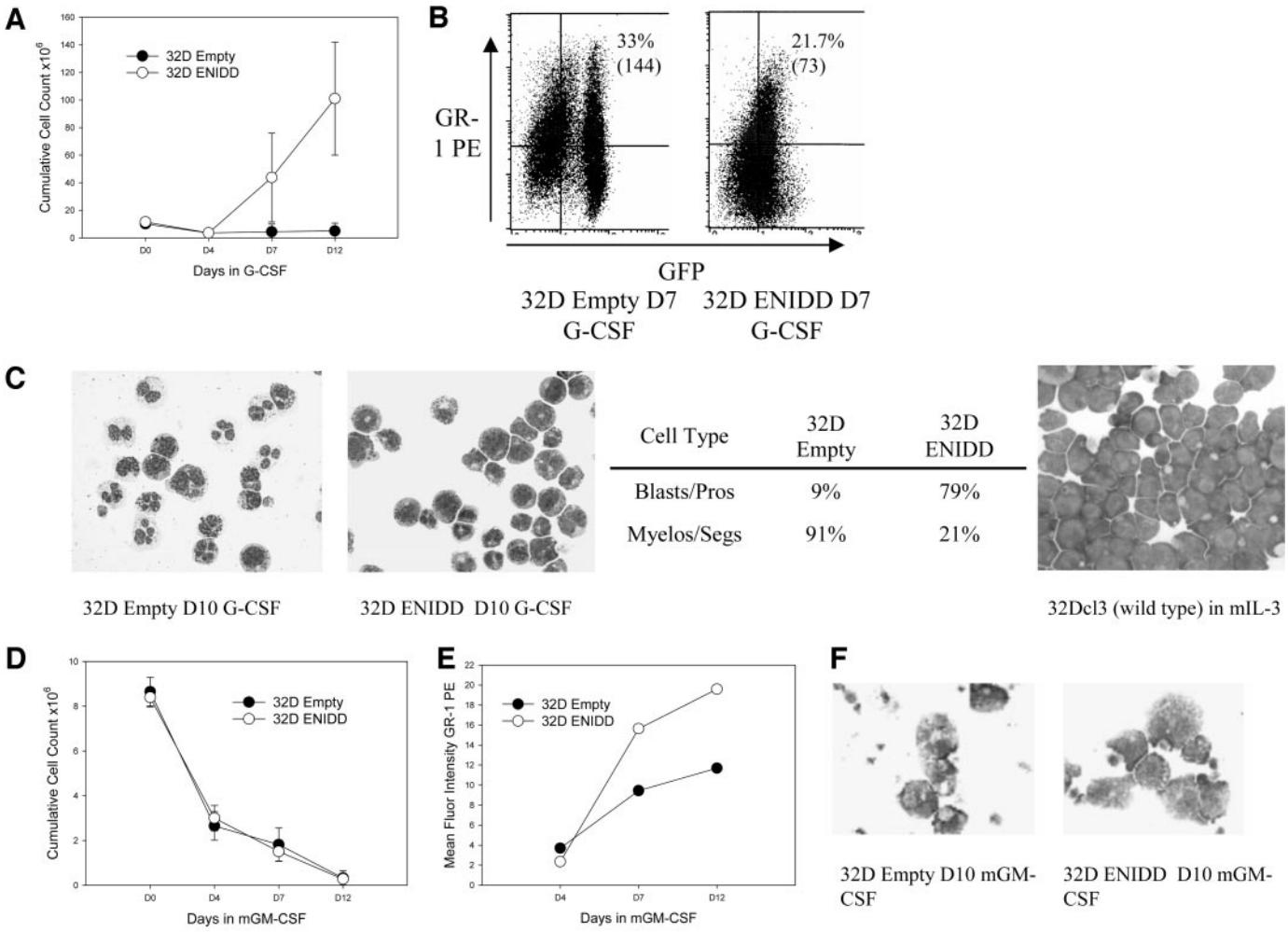

Fig. 5. ENIDD prevents terminal granulocyte but not macrophage differentiation of 32Dcl3 cells. To competitively inhibit endogenous ETO interaction with N-CoR, ENIDD was expressed in 32Dcl3 cells (*32D ENIDD*). Control cells were transfected with empty vector (*32D Empty*). Stable transfectants were selected in G418 and sorted for GFP + by fluorescence-activated cell sorting. *A*, cell counts of 32D Empty and 32D ENIDD in G-CSF (mean ± SD of three independent experiments using independently generated polyclonal populations). *B*, GR-1 PE expression (a murine differentiation marker that increases with granulocyte or monocyte differentiation) on 32D Empty and 32D ENIDD at D7 of culture in G-CSF. The *numbers* represent the percentage of live cells by forward-scatter side scatter that are GR-1 positive with the mean fluorescence intensity GR1-PE expression of the YFP-positive cells in parentheses. *C*, Giemsa-stained cytospin preparations of 32D Empty and 32D ENIDD after 10 days of culture in G-CSF (magnification, ×400) with the differential count of 200 cells; *blasts/pros*, myeloblasts/promyelocytes; *myelos/seg*, myelocytes and metamyelocytes/bands and segmented neutrophils. 32Dcl3 wild-type cells in mIL-3 are shown for comparison. *D*, 32D Empty and 32D ENIDD cell counts in mGM-CSF (mean ± SD of three independent experiments using independently generated polyclonal populations). *E*, representative GR-1 PE expression on 32D Empty and 32D ENIDD in mGM-CSF at the indicated time points. *F*, 32D Empty and 32D ENIDD Giemsa-stained cytospin preparations after 10 days of culture in mGM-CSF (magnification, ×630).

Expression of ENIDD in 32Dcl3 Cells Prevents Terminal Granulocyte but not Macrophage Differentiation. To examine the consequences of disrupting endogenous ETO-2 interactions with N-CoR on myeloid differentiation, we expressed ENIDD in 32Dcl3 cells. Stable transfectants were selected in G418 and then sorted for GFP positivity. 32Dcl3 cells transfected with ENIDD (32D ENIDD) or pIRES-myc-nuc-EGFP2 (32D Empty) were cultured in G-CSF or mGM-CSF. In G-CSF, 32D Empty undergo terminal differentiation into neutrophils as demonstrated by increased GR-1 expression on flow cytometry and on cytospin preparations (Fig. 5, *A–C*). In contrast, 32D ENIDD continue to proliferate in G-CSF (Fig. 5*A*). 32D ENIDD did demonstrate some increase in GR-1 expression, and although abundant granule formation was noted on examination of Giemsa-stained cytospin preparations, there was a marked decrease in terminal differentiation into neutrophils (Fig. 5, *B* and *C*). In mGM-CSF, both 32D Empty and 32D ENIDD terminally differentiate into macrophages (Fig. 5, *D–F*). The inhibition of differentiation in G-CSF but not in mGM-CSF is similar to the effect noted with expression of full-length AML1-ETO in 32Dcl3 cells. Experiments were performed three times using independently generated polyclonal populations of stable transfectants.

In mIL-3, there is no difference in the proliferation rate or GR-1 expression between 32D Empty and 32D ENIDD (data not shown).

Expression of ENIDD Blocks Granulocyte and Increases Macrophage Differentiation of Human CD34-Positive Cord Blood Cells. hCD34+ cord blood cells were transduced with MSCV-IRES-YFP (CD34 Empty) or MSCV-ENIDD-IRES-YFP (CD34 ENIDD). YFP-positive cells (ENIDD and YFP are translated from the same mRNA transcript) were flow sorted and then cultured in IMDM 20% fetal bovine serum containing IL-3, stem cell factor, and G-CSF to promote granulocyte differentiation. CD34 Empty underwent terminal differentiation into neutrophils with increased CD11b myeloid differentiation marker expression and abundant segmented forms on Giemsa-stained cytospin preparations (Fig. 6, *A* and *B*). In contrast, there was less CD11b expression and no terminal granulocyte differentiation of CD34 ENIDD on examination of Giemsa-stained cytospin preparations (Fig. 6, *A* and *B*). However, CD34 ENIDD did undergo terminal differentiation into macrophages: CD13 expression [CD13 is

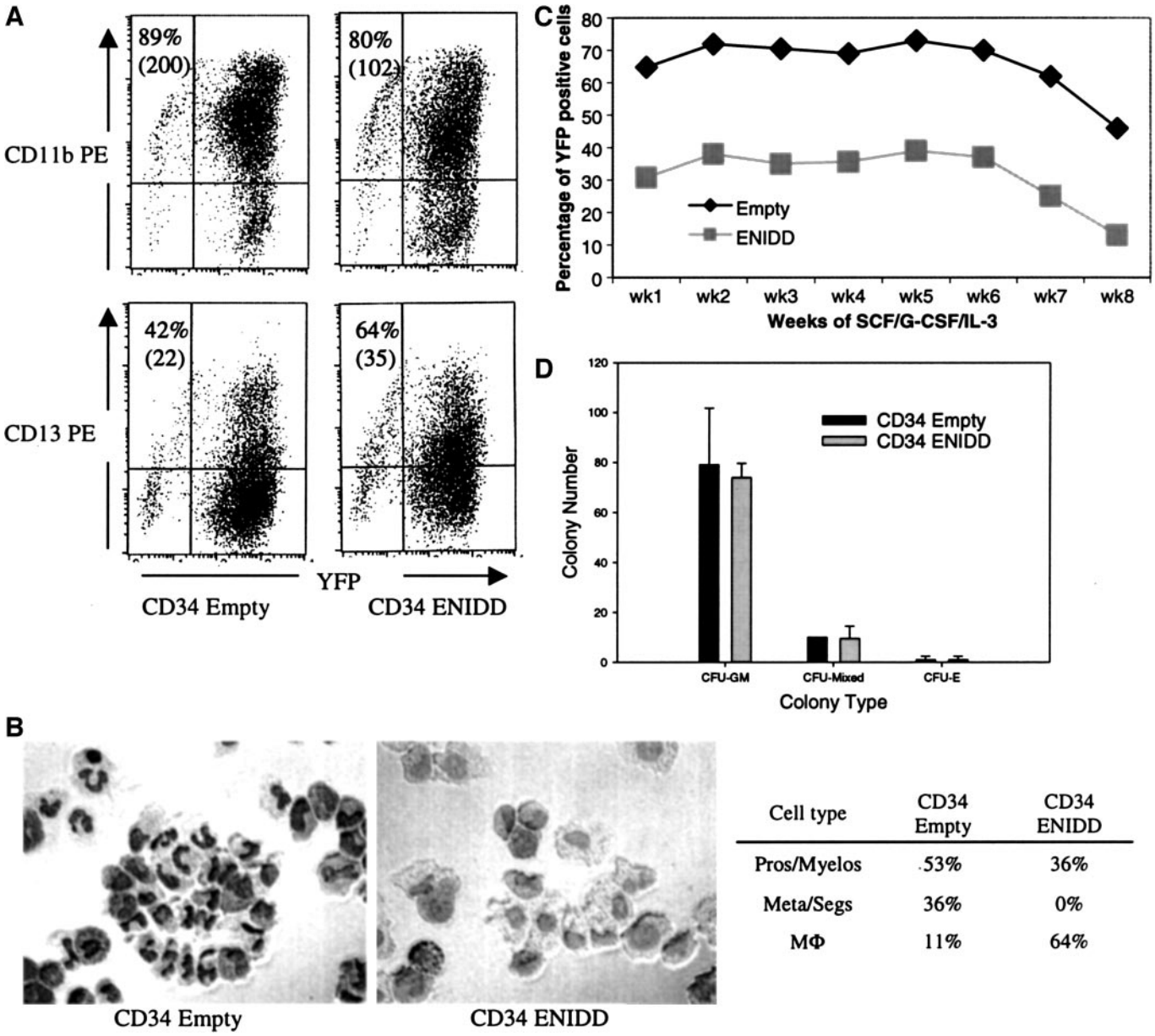

Cell type	CD34 Empty	CD34 ENIDD
Pros/Myelos	53%	36%
Meta/Segs	36%	0%
MΦ	11%	64%

Fig. 6. ENIDD prevents terminal granulocyte but not macrophage differentiation of human CD34+ hematopoietic cells. Human CD34+ cord blood cells transduced with empty vector (*CD34 Empty*) or ETO MYND zinc finger (*CD34 ENIDD*) were analyzed for growth and differentiation characteristics after 15 days of culture in IMDM 20% FBS, stem cell factor, G-CSF, and IL-3. Successfully transduced cells were YFP positive (an IRES-YFP vector backbone was used). *A*, CD11b PE and CD13 PE differentiation marker expression. *Numbers* represent the percentage of YFP-positive cells that are PE positive. Mean fluorescence intensity PE expression is in parentheses. Both CD11b and CD13 expression increase with both neutrophil and macrophage differentiation. However, monocytic differentiation is associated with greater CD13 expression. *B*, Giemsa-stained cytospin preparations (magnification, ×400). Segmented neutrophils are seen in CD34 Empty but not in CD34 ENIDD. Differential count of 300 cells; *pros*, promyelocytes; *myelos*, myelocytes; *meta*, metamyelocytes and bands; *segs*, segmented neutrophils; *MΦ*, macrophages. *C*, a graph of the percentage of CD34 Empty and CD34 ENIDD cells that remained YFP positive over time during culture of transduced but unsorted cells. An MSCV-IRES vector was used to transduce the cells so that both YFP and ENIDD (in the case of ENIDD transduction) are translated from the same mRNA transcript. The YFP-positive cells did not demonstrate a proliferative advantage over the YFP negative cells. *D*, mean numbers of CFU-GM (granulocyte-macrophage), CFU-mixed, and CFU-E (erythroid) formed by YFP-positive CD34 Empty *versus* YFP-positive CD34 ENIDD cells (colony count at day 15 of methylcellulose culture).

seen on both granulocytes and monocytes; monocytic differentiation is associated with greater CD13 expression (19)] and the percentages of macrophages were higher in CD34 ENIDD compared with CD34 Empty (Fig. 6, *A* and *B*).

In culture of transduced but unsorted cells, the proportion of YFP-positive cells did not appreciably increase or decrease in either the empty vector or ENIDD retroviral supernatant treated populations. This suggested that ENIDD expression did not confer a proliferative advantage (or disadvantage) on human cord blood cells over this time period (Fig. 6*C*).

At day 15 of methylcellulose culture, there was no difference in the number or size of CFU-GM, CFU-mixed, CFU-E, or BFU-E derived from CD34 Empty *versus* CD34 ENIDD (Fig. 6*D*).

Similar to the effects of ENIDD noted in 32Dcl3 cells, ENIDD prevents terminal neutrophil but not macrophage differentiation of hCD34+ hematopoietic cells.

DISCUSSION

ETO-2, a member of the ETO family of proteins, is expressed in both murine and human hematopoietic cells. Using reverse transcription-PCR, we did not detect ETO expression in either murine

32Dcl3 granulocyte/macrophage progenitors or in human CD34+ hematopoietic cells. ETO-2, like ETO (and AML1-ETO), interacts with the ubiquitous corepressor N-CoR. Because both ETO-2 and AML1-ETO are likely to bind to the same site on N-CoR, we examined whether AML1-ETO decreased ETO-2 interactions with N-CoR. AML1-ETO decreases the coimmunoprecipitation of ETO-2 with N-CoR in 293-T cells. Furthermore, ETO-2 overexpression relieved AML1-ETO-induced granulocyte differentiation arrest of 32Dcl3 cells in G-CSF. This suggested that inhibition of endogenous ETO-2 interactions with N-CoR may be one mechanism by which AML1-ETO could impair granulocyte differentiation. The MYND domain present in the ETO family is necessary for interactions with N-CoR (3–7). To examine the effect of inhibiting endogenous ETO-2 interactions with N-CoR without other effects of AML1-ETO such as direct interference with AML1 transactivation (17, 20), we determined whether the MYND domain of ETO could act as an ENIDD by binding to N-CoR and specifically antagonizing ETO-2 interactions with N-CoR. This was confirmed in 293T cells in which ENIDD coimmunoprecipitated with N-CoR and specifically decreased the bidirectional coimmunoprecipitation of ETO-2 with N-CoR but not of the RAR with N-CoR. To examine the functional role of endogenous ETO-2 interactions with endogenous N-CoR, we expressed ENIDD in 32Dcl3 murine granulocyte/macrophage progenitors and human CD34+ cells. ENIDD prevented terminal granulocyte but not macrophage differentiation, an effect similar to that seen with full-length AML1-ETO expression in 32Dcl3 cells. These results suggest that endogenous ETO-2 interactions with N-CoR have a usual role in facilitating granulocyte differentiation and that one mechanism by which AML1-ETO impairs granulocyte differentiation is through disruption of this interaction.

ETO-2 has multiple protein interactions and may have multiple cellular functions besides those mediated via interactions with N-CoR. By sequestering ETO-2 (16), AML1-ETO may disrupt a number of usual ETO-2 interactions. ENIDD only mimics the effect of disrupting ETO-2 interactions with N-CoR and may underestimate the contribution of disrupted ETO-2 activity to the abnormal hematopoiesis in AML1-ETO leukemia.

A decrease in the proportion of terminally differentiated granulocytes and an increase in the proportion of macrophages in the hCD34+ ENIDD cultures could arise through increased macrophage commitment of the common granulocyte/macrophage progenitor (causing a relative decrease in granulocytes) or inhibition of terminal granulocyte differentiation after granulocyte commitment by the common progenitor. Although the CD34 ENIDD culture system lacked terminally differentiated neutrophils, it did contain numerous granulated cells with promyelocyte morphology. This suggests that ENIDD inhibits terminal granulocyte differentiation after granulocyte commitment by the common progenitor. Similarly, 32D ENIDD in G-CSF continues to proliferate with a morphology of partial granulocyte differentiation. However, based on our current data, we cannot rule out the possibility that ENIDD also promotes macrophage commitment of bipotential granulocyte/macrophage progenitors.

In addition to the ETO family members ETO, ETO-2, and MTGR1(2), there are at least four other proteins in humans and mice that have been identified as containing the MYND domain (SET and MYND domain-containing 3; melanin-concentrating hormone receptor interacting zinc finger protein; protein kinase C-binding protein RACK7; and zinc finger, MYND domain-containing 10). Therefore, we cannot exclude the possibility that some or all of the AML1-ETO- or ENIDD-induced effect is related to interference with protein-protein interactions involving other MYND domain-containing proteins. Nonetheless, the relief of AML1-ETO-induced granulocyte differentiation arrest by overexpression of ETO-2 suggests the effects are related to inhibition of ETO-2 interactions with N-CoR.

AML1-ETO does not prevent macrophage differentiation of 32Dcl3 cells. AML1-ETO expression in primary murine hematopoietic stem cells also did not prevent terminal macrophage differentiation, although it did prevent terminal granulocyte differentiation (21). AML1-ETO up-regulates transcription of the macrophage colony-stimulating factor (M-CSF) receptor (22). In primary human cells transduced with AML1-ETO, there was an increase in CD14 expression indicating macrophage differentiation (23). Treatment of the AML1-ETO-containing human cell-line Kasumi-1 with the histone deacetylase inhibitor phenylbutyrate resulted in monocytoid differentiation (24). These findings suggest that both murine and human AML1-ETO-containing cells may be amenable to macrophage differentiation. This may be a feature that can be exploited for therapeutic purposes.

In conclusion, AML1-ETO inhibits the interaction between ETO-2 and N-CoR. The functional consequence of disrupting ETO-2 interactions with N-CoR in hematopoietic cells is impaired granulocyte but not macrophage differentiation. AML1-ETO inhibition of endogenous ETO-2 interactions with N-CoR may be one mechanism by which the leukemia fusion protein impairs granulocyte differentiation.

ACKNOWLEDGMENTS

Flag-N-CoR vector was a kind gift of Michael Rosenfeld. ETO-2 vector was a kind gift of Ari Melnick. RAR vector was a kind gift of Kun-Sang Chang. Giuseppina Nucifora and Johnson Liu provided valuable advice and discussions. We thank Alvin Ayala, Annette Bruno, John McGuire, Michael J. Pacini, Paul Weiss, and Karen Hagen for technical assistance.

REFERENCES

1. Davis JN, Williams BJ, Herron JT, Galiano FJ, Meyers S. ETO-2, a new member of the ETO-family of nuclear proteins. Oncogene 1999;18:1375–83.
2. Kitabayashi I, Ida K, Morohoshi F, et al. The AML1-MTG8 leukemic fusion protein forms a complex with a novel member of the MTG8(ETO/CDR) family, MTGR1. Mol Cell Biol 1998;18:846–58.
3. Hildebrand D, Tiefenbach J, Heinzel T, Grez M, Maurer AB. Multiple regions of ETO cooperate in transcriptional repression. J Biol Chem 2001;276:9889–95.
4. Wang J, Hoshino T, Redner RL, Kajigaya S, Liu JM. ETO, fusion partner in t(8;21) acute myeloid leukemia, represses transcription by interaction with the human N-CoR/mSin3/HDAC1 complex. Proc Natl Acad Sci USA 1998;95:10860–5.
5. Lutterbach B, Westendorf JJ, Linggi B, et al. ETO, a target of t(8;21) in acute leukemia, interacts with the N-CoR and mSin3 corepressors. Mol Cell Biol 1998;18:7176–84.
6. Gelmetti V, Zhang J, Fanelli M, Minucci S, Pelicci PG, Lazar MA. Aberrant recruitment of the nuclear receptor corepressor-histone deacetylase complex by the acute myeloid leukemia fusion partner ETO. Mol Cell Biol 1998;18:7185–91.
7. Lutterbach B, Sun D, Schuetz J, Hiebert SW. The MYND motif is required for repression of basal transcription from the multidrug resistance 1 promoter by the t(8;21) fusion protein. Mol Cell Biol 1998;18:3604–11.
8. Amann JM, Nip J, Strom DK, et al. ETO, a target of t(8;21) in acute leukemia, makes distinct contacts with multiple histone deacetylases and binds mSin3A through its oligomerization domain. Mol Cell Biol 2001;21:6470–83.
9. Horlein AJ, Naar AM, Heinzel T, et al. Ligand-independent repression by the thyroid hormone receptor mediated by a nuclear receptor co-repressor. Nature 1995;377:397–404.
10. Alland L, Muhle R, Hou H Jr, et al. Role for N-CoR and histone deacetylase in Sin3-mediated transcriptional repression. Nature 1997;387:49–55.
11. Bauer A, Mikulits W, Lagger G, Stengl G, Brosch G, Beug H. The thyroid hormone receptor functions as a ligand-operated developmental switch between proliferation and differentiation of erythroid progenitors. EMBO J 1998;17:4291–303.
12. Du C, Redner RL, Cooke MP, Lavau C. Overexpression of wild-type retinoic acid receptor α (RARα) recapitulates retinoic acid-sensitive transformation of primary myeloid progenitors by acute promyelocytic leukemia RARα-fusion genes. Blood 1999;94:793–802.
13. Kastner P, Lawrence HJ, Waltzinger C, Ghyselinck NB, Chambon P, Chan S. Positive and negative regulation of granulopoiesis by endogenous RARα. Blood 2001;97:1314–20.

14. Gamou T, Kitamura E, Hosoda F, et al. The partner gene of AML1 in t(16;21) myeloid malignancies is a novel member of the MTG8(ETO) family. Blood 1998; 91:4028–37.
15. Westendorf JJ, Yamamoto CM, Lenny N, Downing JR, Selsted ME, Hiebert SW. The t(8;21) fusion product, AML-1-ETO, associates with C/EBP-α, inhibits C/EBP-α-dependent transcription, and blocks granulocytic differentiation. Mol Cell Biol 1998; 18:322–33.
16. Lindberg SR, Olsson A, Persson AM, Olsson I. Interactions between the leukaemia-associated ETO homologues of nuclear repressor proteins. Eur J Haematol 2003;71: 439–47.
17. Hwang ES, Hong JH, Bae SC, Ito Y, Lee SK. Regulation of c-fos gene transcription and myeloid cell differentiation by acute myeloid leukemia 1 and acute myeloid leukemia-MTG8, a chimeric leukemogenic derivative of acute myeloid leukemia 1. FEBS Lett 1999;446:86–90.
18. Wang J, Hoshino T, Redner RL, Kajigaya S, Liu JM. ETO, fusion partner in t(8;21) acute myeloid leukemia, represses transcription by interaction with the human N-CoR/mSin3/HDAC1 complex. Proc Natl Acad Sci USA 1998;95:10860–5.
19. Laouar A, Wietzerbin J, Bauvois B. Divergent regulation of cell surface protease expression in HL-60 cells differentiated into macrophages with granulocyte macrophage colony stimulating factor or neutrophils with retinoic acid. Int Immunol 1993;5:965–73.
20. Linggi B, Muller-Tidow C, Van De LL, et al. The t(8;21) fusion protein, AML1 ETO, specifically represses the transcription of the p14(ARF) tumor suppressor in acute myeloid leukemia. Nat Med 2002;8:743–50.
21. de Guzman CG, Warren AJ, Zhang Z, et al. Hematopoietic stem cell expansion and distinct myeloid developmental abnormalities in a murine model of the AML1-ETO translocation. Mol Cell Biol 2002;22:5506–17.
22. Rhoades KL, Hetherington CJ, Rowley JD, et al. Synergistic up-regulation of the myeloid-specific promoter for the macrophage colony-stimulating factor receptor by AML1 and the t(8;21) fusion protein may contribute to leukemogenesis. Proc Natl Acad Sci USA 1996;93:11895–900.
23. Mulloy JC, Cammenga J, MacKenzie KL, Berguido FJ, Moore MA, Nimer SD. The AML1-ETO fusion protein promotes the expansion of human hematopoietic stem cells. Blood 2002;99:15–23.
24. Wang J, Saunthararajah Y, Redner RL, Liu JM. Inhibitors of histone deacetylase relieve ETO-mediated repression and induce differentiation of AML1-ETO leukemia cells. Cancer Res 1999;59:2766–9.